ChemPubSoc Europe

DOI: 10.1002/cctc.201500501

CHEMCATCHEM Full Papers

Highly Selective Copper Catalyst Supported on Mesoporous Carbon for the Dehydrogenation of Ethanol to Acetaldehyde

Qing-Nan Wang, Lei Shi, and An-Hui Lu*[a]

The dehydrogenation of ethanol to acetaldehyde is of great importance in synthetic chemistry and the fine chemical industry. In this study, we report that a mesoporous-carbon-supported Cu catalyst exhibited a high reaction rate and excellent product selectivity in ethanol dehydrogenation to acetaldehyde. Under the severe conditions of an ethanol concentration of 15 vol% and a gaseous hourly space velocity of 8600 h^{-1}, the Cu-based carbon catalyst maintains a conversion of ≈73% and an acetaldehyde selectivity of ≈94% at 553 K. Meanwhile, a prominent space time yield (225 h^{-1}) of acetaldehyde is obtained, which is far higher than that (112 h^{-1}) on the mesoporous-SBA-15-supported Cu catalyst. Ethanol adsorption studies prove that the enrichment of the carbon support for reactants makes a contribution to the high reaction rate. Importantly, kinetic measurements indicate that the scarce surface groups of the mesoporous carbon support minimize the secondary reactions of acetaldehyde, which are generally catalyzed by –OH and/or –COOH on the surface of the support as exemplified by the mesoporous-SBA-15-supported Cu catalyst. This accounts for the excellent selectivity toward acetaldehyde on the mesoporous-carbon-supported Cu catalyst. Therefore, these surface characteristics of the carbon support show great advantages in this dehydrogenation reaction.

Introduction

The increase of alternative energy produced from renewable biomass and its derivatives helps to alleviate our dependence on fossil resources.[1,2] Ethanol, which is obtained easily from biomass fermentation,[3] is particularly attractive because of its increased annual production and low cost.[4,5] In synthetic chemistry and the fine chemical industry, ethanol is utilized widely for the production of hydrogen, acetic acid, 1-butanol, ethyl acetate, 1,3-butadiene, acetaldehyde, and other chemicals.[4,6–12] In particular, acetaldehyde, a significant bulk chemical, is valuable for the production of peracetic acid, pentaerythritol, pyridine bases, butanediol, and trichloroacetic aldehyde, with a worldwide production over 10^6 tons per year.[13,14]

As hydrogen is the sole byproduct, the dehydrogenation of ethanol to acetaldehyde (DHEA)[11,12,15] represents an atom-economic process,[8,9,16] which is a more favorable and green alternative to the current Wacker process of oxidation ethylene to make acetaldehyde using $PdCl_2$ and $CuCl_2$ as catalysts in strong acidic solutions.[4] Currently, in industrial production and literature reports, SiO_2-supported Cu catalysts are mainly used in DHEA because of the nearly neutral surface of SiO_2 compared with Al_2O_3, ZnO, and ZrO_2. However, the selectivity towards acetaldehyde is not entirely satisfactory.[12,17–19] The low selectivity is a fatal result of secondary reactions, that is, aldolization and ketonization,[20–22] which are generally catalyzed by acid and/or base sites on the support surface.[10] Hence, there is still a desire to develop new catalysts that have a notable selectivity to acetaldehyde during DHEA.

Compared with conventional oxides, for example, SiO_2 and Al_2O_3, carbon materials possess a chemically inert nature[23,24] and intrinsically hydrophobic properties.[25–27] The surface inertness of the carbon material may inhibit the secondary reactions of DHEA, and the hydrophobic surface probably exhibits a potential enrichment ability for organic molecules, such as ethanol. Moreover, mesoporous carbons (MCs) possess a fully interconnected mesoporosity, which favors the dispersion of active components and diffusion of reactants.[25,28] Consequently, it can be envisaged that if such an MC-supported Cu catalyst is used for DHEA, excellent selectivity might be achieved. To the best of our knowledge, there has been little research on the use of MC-supported Cu catalysts for DHEA.

In this paper, we selected MC as the support for the preparation of Cu catalysts and studied its catalytic performance for DHEA. In comparison, a mesoporous silica SBA-15-supported Cu catalyst (Cu/SBA-15) was evaluated for DHEA. It was found that MC-supported catalysts exhibited excellent acetaldehyde selectivity of 94.1% and a space time yield of 225 h^{-1} at 553 K under a gaseous hourly space velocity (GHSV) of 8600 h^{-1}. Furthermore, the influence of the enrichment ability of the sup-

[a] Q.-N. Wang,[+] Dr. L. Shi,[+] Prof. A.-H. Lu
The State Key Laboratory of Fine Chemicals
School of Chemical Engineering
Dalian University of Technology
Dalian 116024 (P.R. China)
Fax: (+86) 411-84986112
E-mail: anhuilu@dlut.edu.cn

[+] These authors contributed equally to this work.

Supporting information for this article is available on the WWW under http://dx.doi.org/10.1002/cctc.201500501.

This publication is part of a Special Issue on "Carbon in the Catalysis Community". Once the full issue has been assembled, a link to its Table of Contents will appear here.

port for the reactant on the reaction rate was investigated. Combined with kinetic measurements, the origin of the high selectivity to acetaldehyde on Cu/MC was elucidated.

Results and Discussion

Physicochemical properties of the catalysts

The precursors of the Cu/MC and Cu/SBA-15 catalysts were prepared by the incipient wetness impregnation of $Cu(NO_3)_2$ aqueous solution (see details in the Experimental Section). The physicochemical properties of the fresh catalysts are reported in Table 1 and Figures 1 and 2. Highly dispersed metallic Cu tends to be oxidized to high-valence oxide upon exposure to the ambient atmosphere. Thus, in situ XRD characterization (Figure 1 a) was adopted to investigate the phase evolution of Cu/MC catalysts under 5 vol% H_2/Ar as a function of the reduction temperature. Diffraction peaks at $2\theta = 43.3$, 50.4, and 74.1° became observable because some Cu^{2+} species on the Cu/MC catalysts precursor were reduced to metal Cu if the reduction temperature was ramped to 523 K. According to the JCPDS card 04-0836, these diffraction peaks correspond to the specific (111), (200), and (220) crystal planes of Cu, respectively. In thermodynamic terms, there is little energy difference between the different low-index faces, so Cu metal is liable to form multifaceted crystalline surfaces.[29] This result indicates that only metallic Cu is visible after hydrogen treatment, which is consistent with the result of Choi and Vannice.[29] With a further increase of the reduction temperature to 823 K, the Cu particle size increases slightly from 13.4 to 14.1 nm, which is calculated by the Scherrer equation using the Cu (111) reflection. The particle size obtained at the reduction temperature of 723 K for 2 h is presented in the Table 1. For the Cu/SBA-15 catalyst after reduction at 723 K, only an amorphous diffraction peak that ranges from approximately 15 to 35° is detected, therefore, neither the peaks of metallic Cu nor copper oxide appear (Figure S1 a). This agrees with the results of Zhao et al. on Cu/SiO_2.[30] The crystallite size of the Cu on this catalyst may be quite small (below the detection limit of XRD) or metallic Cu is oxidized to a higher valence and, spontaneously, to a monolayer dispersion[31] upon exposure to air during analysis.

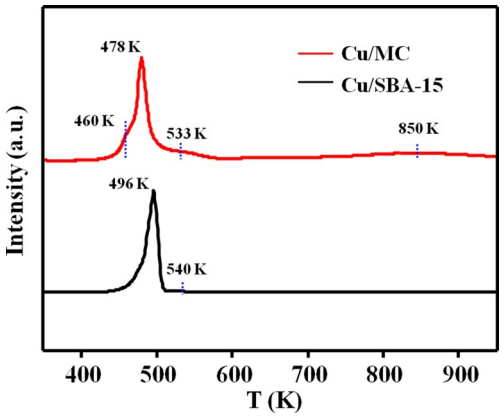

Figure 2. H_2-TPR profiles of Cu/MC and Cu/SBA-15.

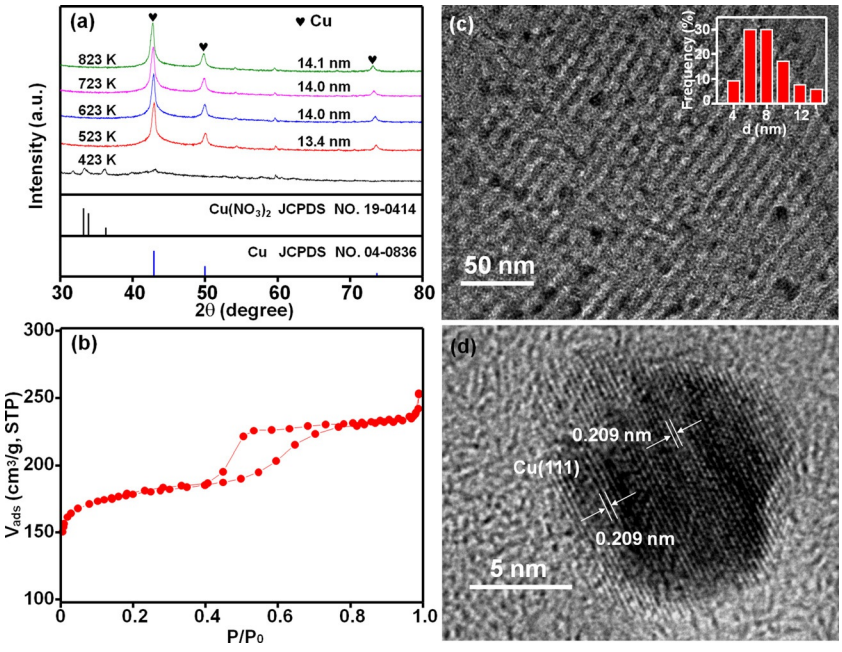

Figure 1. a) In situ XRD patterns, b) N_2 sorption isotherm, and c and d) TEM images of the Cu/MC catalyst.

Table 1. Structure parameters of the bare supports and the supported Cu catalysts after reduction.

Catalyst	Cu loading [wt%]	S_{BET} [$m^2 g^{-1}$]	V_{total} [$cm^3 g^{-1}$]	D_p [nm]	Particle size [nm] XRD	TEM	N_2O	Dispersion of Cu[a] [%]	Cu surface[a] [$m^2_{Cu} g_{Cu}^{-1}$]
MC	0	532	0.38	5.8	–	–	–	0	0
Cu/MC	10	545	0.35	4.4	9.3	14.0	16.2	7.0	47.2
SBA-15	0	815	1.03	7.9	–	–	–	0	0
Cu/SBA-15	10	470	0.83	6.8	ND[b]	ND	9.8	11.5	78.1

[a] Dispersion and surface of Cu were determined by N_2O surface oxidation and H_2-TPR titration. [b] ND, not detected.

The porous structure and surface area of these samples were analyzed by N_2 sorption measurements at 77.4 K. The nitrogen sorption isotherm of the Cu/MC catalyst is of type IV in shape, which represents a typical mesoporous structure (Figure 1b and Figure S1b). The Cu/SBA-15 sample also shows a type IV isotherm, which is the same as that of the bare support.[32]

The morphologies and structural details of the Cu/MC catalyst were examined using TEM. The dark metal nanoparticles assignable to Cu are highly dispersed in the mesopores of the MC (Figure 1c and d and Figure S2). The inset statistical histogram shows a narrow particle size distribution with an average Cu nanoparticle size of approximately 9.3 nm, which is smaller than that (≈20 nm) of Cu/carbon nanofibers.[33] This is in line with the results obtained from the in situ XRD patterns. It was also reported that the reduction of CuO/C can partially remove the anchoring groups from the carbon support to yield CO_2 or CO, which results in increased Cu particle sizes.[34] High-resolution transmission electron microscopy (HRTEM) shows that the Cu particles have a *d* spacing of ≈0.209 nm, which corresponds to the Cu (111) plane. This is consistent with the results of in situ XRD (Figure 1a), which includes only a small proportion of (200) and (220) planes.

The structural parameters of Cu/MC and Cu/SBA-15 are summarized in Table 1. The surface area and pore volume of Cu/MC are almost the same as those of the bare support. However, the pore diameter decreases from 5.8 to 4.4 nm. The surface area, pore volume, and pore size of Cu/SBA-15 are dramatically decreased compared to those of the support, for example, the surface area is reduced from 815 to 470 m^2g^{-1}. This implies that most of the deposited Cu component is filled into the mesopores of the SBA-15 support. The average particle sizes of the catalysts determined by N_2O chemisorption, in situ XRD, and TEM are also presented in Table 1. If we assume that the Cu particles are spherical, the dispersion (*D*) of Cu on the Cu/MC catalyst is 7.0%, which is lower than that (11.5%) of Cu/SBA-15. Therefore, the Cu size of Cu/MC calculated by the chemisorption of N_2O is larger than that on Cu/SBA-15.

Hydrogen temperature-programmed reduction (H_2-TPR; Figure 2) was performed to reveal the type of metal species and reducibility of Cu/MC and Cu/SBA-15. For the MC-supported sample, there is a main reduction peak at 478 K, which represents the reduction of Cu^{2+} to Cu. In addition, two shoulder peaks appear at 460 and 533 K. Dandekar et al. reported that surface carboxyl groups on a carbon support were beneficial to render a higher dispersion of Cu.[34] Although MC was obtained by the pyrolysis of the carbon precursors at 1073 K, a small amount of surface groups might remain.[35] Thus, the first shoulder at 460 K is the reduction of highly dispersed Cu particles.[36,37] The H_2 consumption peak at 533 K can be assigned to the reduction of larger cupric oxide particles.[31] The H_2 consumption of these reduction processes are approximately 7.2, 32.6, and 5.3 $mL/g_{catalyst}$, which correspond to the areas of the peaks at 460, 478, and 533 K, respectively. The quantity of H_2 consumed is higher than the theoretical value, approximately 35 $mL/g_{catalyst}$, which indicates the complete reduction of Cu^{2+} to Cu. In addition, another H_2 consumption peak appears gradually for this sample in a relatively high temperature range of 713–950 K. This indicates the alkylation of carbon with H_2 catalyzed by Cu. The etching process enlarged the surface area of the carbon support (Table 1) and favored the exposure of active components to result in metal-porous/hollow carbon catalysts.[38] This special structure might facilitate the diffusion and reaction of reactants in the nanospace around the Cu particles. A further increase of the reduction temperature leads to a decrease of this effect, which then becomes absent as the particle size of Cu becomes larger. For Cu/SBA-15, a sharp reduction peak appears at 496 K with a shoulder at 540 K. This main peak indicates the reduction of dispersed cupreous particles on the silica support.[31,37] The total H_2 uptake of this sample is approximately 41.5 $mL/g_{catalyst}$, which implies the complete reduction of the CuO phase. Moreover, this result also confirms that the active component on MC is reduced easily to Cu under H_2 treatment. The H_2-TPR result is consistent with the above discussion about the particle size distribution and surface area of Cu/MC listed in Table 1.

Catalytic performance of Cu/MC and Cu/SBA-15 catalysts

Ethanol dehydrogenation, catalyzed by Cu catalysts, is known to produce acetaldehyde and hydrogen. However, byproducts of ethyl acetate, methyl ethyl ketone, acetone, butanal, and butanol[10,12,17–19] are also generated as a result of the further reaction of acetaldehyde catalyzed by the acid and/or base sites of the supports.[10,17] The results for the catalysis of DHEA are compiled in Table 2 and Figures 3 and 4.

Under a GHSV of 26000 h^{-1} and 553 K (Table 2), there is a slight difference between these two catalysts in terms of

Table 2. Catalytic results for ethanol dehydrogenation to acetaldehyde on Cu/MC and Cu/SBA-15.[a]

Catalyst	GHSV [h^{-1}]	Conv. [%]	Rate[b] [s^{-1}]	Selectivity [%][c] AC	EAC	MEK	ACE	Others	Yield[d] [%]	STY[e] [h^{-1}]
Cu/MC	26000	83.0	0.110	95.1	1.7	0.7	0.7	1.8	79.0	258
Cu/SBA-15	26000	90.1	0.070	82.1	8.2	1.3	1.0	7.4	73.9	147
Cu/MC	8600	72.7	0.096	94.0	3.0	1.4	0.6	1.0	68.4	225
Cu/SBA-15	8600	82.8	0.064	68.1	11.7	2.0	0.7	16.1	56.4	112

[a] Reaction conditions: catalyst 0.100 g, $WHSV_{C_2H_5OH}$ = 2.4 h^{-1}, N_2 40 or 10 mL min^{-1}, 553 K. [b] Rate represents the reaction rate of ethanol. [c] AC: acetaldehyde, EAC: ethyl acetate, MEK: methyl ethyl ketone, ACE: acetone, Others: 1-butanol, butanal, and C6+. [d] Yield is calculated as conversion × selectivity/100. [e] STY represents the space time yield of acetaldehyde.

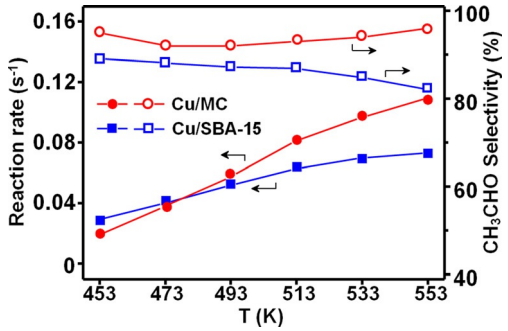

Figure 3. C_2H_5OH reaction rate and CH_3CHO selectivity during dehydrogenation over Cu/MC and Cu/SBA-15 as a function of the reaction temperature. Reaction conditions: catalyst 0.1 g, weight hourly space velocity (WHSV) of $C_2H_5OH = 2.4\ h^{-1}$, N_2 40 mL min^{-1}, $C_2H_5OH/N_2 = 5{:}95$, GHSV = 26 000 h^{-1}.

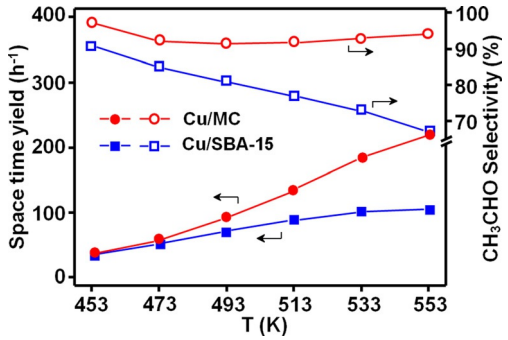

Figure 4. Selectivity and space time yield of CH_3CHO during dehydrogenation over Cu/MC and Cu/SBA-15 as a function of the reaction temperature. Reaction conditions: catalyst 0.1 g, $WHSV_{C_2H_5OH} = 2.4\ h^{-1}$, N_2 10 mL min^{-1}, $C_2H_5OH/N_2 = 15{:}85$.

conversion, 83.0% for Cu/MC and 90.1% for Cu/SBA-15. To reflect the real catalytic efficiency of these two catalysts, the reaction rate is calculated as the amount of ethanol converted [mmol] per the amount of surface Cu [mmol] obtained from the metal dispersion [s^{-1}] at each reaction temperature. The comparison of reaction rates on these catalysts is shown in Figure 3. Cu/MC shows a higher reaction rate than Cu/SBA-15 above 473 K. This superiority becomes clearer as the reaction temperature increases, 0.11 versus 0.07 s^{-1} at 553 K. According to literature reports,[12,17–19] Cu is the active center for this DHEA. Although Cu/MC possesses a lower Cu dispersion than Cu/SBA-15 (Table 1), it shows an excellent reaction rate for ethanol. So, to shed light on this phenomenon, the effect of the support characteristics on the catalytic performance is considered.

If we consider the enrichment ability of hydrophobic carbon for organic reactants, the adsorption experiments of ethanol on MC and SBA-15 were conducted (Figure S3). The results show that the carbon surface has a higher ethanol concentration than the silica surface. The reaction order of DHEA with respect to ethanol is approximately 0.5 (Figure S4), therefore, a high density distribution of ethanol molecules on the carbon surface accelerates the reaction rate. As a result of the lower Cu dispersion of Cu/MC than that of Cu/SBA-15, at temperatures below 473 K the reaction rate of Cu/MC is lower than that of Cu/SBA-15. At temperatures above 473 K, with a decreased reactant concentration, the collision frequency between ethanol and active sites may be high, for which the enrichment of the carbon support for the reactants contributes to the high reaction rate. In view of the selectivity of acetaldehyde, Cu/MC is better than Cu/SBA-15, especially at a high reaction temperature, for example, at 553 K the selectivity of Cu/MC is 95.1%, whereas that of Cu/SBA-15 is 82.1% (Figure 3). For catalytic reactions, the selectivity to the target products is of importance. Although the Cu/MC catalyst has a lower Cu dispersion than Cu/SBA-15, excellent acetaldehyde selectivity and reaction rate are obtained. These exciting results show that MC is a potential support for the preparation of active Cu-based catalysts for DHEA. A comparative summary of the literature on ethanol dehydrogenation is listed in Table 3, which supports the extraordinary activity of our carbon-supported catalyst described here. This summary likewise presents what is known about SiO_2-based catalysts to aggravate side reactions in ethanol dehydrogenation.

Table 3. Comparison of the catalytic performance of Cu/MC and Cu catalysts reported in the literature.

Catalyst	Cu [wt%]	T [K]	Conv. [%]	Select. [%]	Yield [%]	Ref.
Cu/MC[a]	10	553	83.0	95.1	78.9	This work
Cu/SiO_2	30	493	76.1	21.0	16.4	[12]
Cu/SiO_2	14.4	673	80.0	85.0	68.0	[17]
		553	22.2	90.1	19.8	
Cu/SiO_2	10	553	53.1	61.0	32.7	[18]
Cu/SiO_2	10	498	41.0	87.2	35.6	[19]

[a] Reaction conditions: catalyst 0.1 g, $WHSV_{C_2H_5OH} = 2.4\ h^{-1}$, N_2 40 mL min^{-1}, $C_2H_5OH/N_2 = 5{:}95$.

Moreover, to explore the advantages of carbon-supported Cu catalysts on product selectivity, more extreme reaction conditions were investigated, for example, a lower GHSV of 8600 h^{-1} and a higher ethanol concentration of 15 vol%. The selectivity and space time yield of acetaldehyde are shown in Figure 4. The space time yield of acetaldehyde was defined as the mass of acetaldehyde [g] formed per mass of surface Cu [g] calculated from the Cu dispersion in 1 h [h^{-1}] at each reaction temperature. A selectivity of 94% retained almost constant from 473 to 553 K. However, for Cu/SBA-15, it showed an inverse proportional function between the selectivity and the reaction temperature, and its selectivity was as low as approximately 68% at 553 K. Therefore, the space time yield of the carbon-supported Cu catalyst is approximately twice as high as that of Cu/SBA-15 at 553 K, which is accordingly 225 and 112 h^{-1}. These results further demonstrate that MC is a favorable alternative to silica to make highly active catalysts for the dehydrogenation of ethanol.

Kinetic measurements

Generally, the characteristics of the active component have a significant influence on the product distribution. To illuminate the difference in product selectivity over these samples, kinetic measurements were considered. An Arrhenius plot of ethanol reaction rate (Figure 5) allows us to identify that the apparent active energy for the dehydrogenation reaction is 51.9 kJ mol^{-1} for Cu/MC and 54.9 kJ mol^{-1} for Cu/SBA-15. This result implies that there is no difference in the nature of the active sites between the two catalysts. It has been proven that this reaction is structure insensitive.[39–41] Hence, it is apparent that the properties of the supports are the dominant factors that influence the acetaldehyde selectivity. Thus, we deduce that the secondary reactions may be attributed to the selectivity difference between Cu supported on MC and SBA-15.

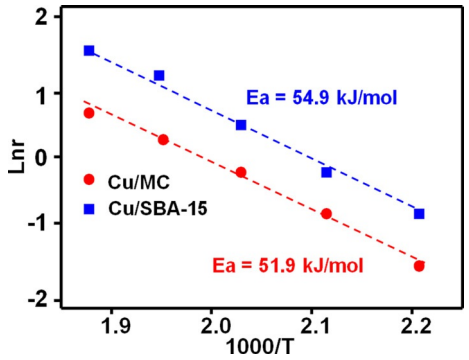

Figure 5. Arrhenius plot of the reaction rate on the Cu/MC and Cu/SBA-15 at 453–533 K. Reaction conditions: catalyst 0.010 g for Cu/MC and 0.005 g for Cu/SBA-15, $WHSV_{C_2H_5OH}$ = 24 or 48 h^{-1}, N_2 40 mL min^{-1}, C_2H_5OH/N_2 = 5:95.

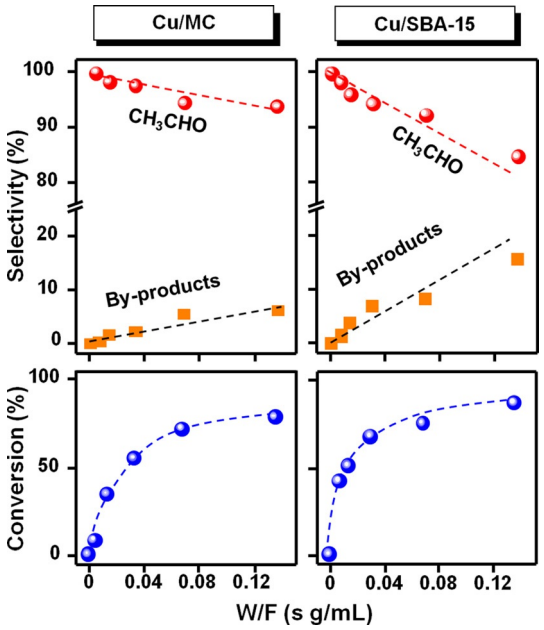

Figure 6. Dependence of product selectivity and ethanol conversion on W/F in the DHEA over a) Cu/MC and b) Cu/SBA-15. Reaction conditions: $WHSV_{C_2H_5OH}$ = 2.4–48 h^{-1}, N_2 40 mL min^{-1}, C_2H_5OH/N_2 = 5:95, 533 K. Byproducts included ethyl acetate, methyl ethyl ketone, acetone, 1-butanol, butanal, and C6+.

To verify the above deduction, the effect of residence time (W/F) on the product selectivity and ethanol conversion over the two catalysts was investigated. With increasing W/F, the selectivity to acetaldehyde decreases from 100 to 95.1% (Figure 6), whereas the selectivity to byproducts increases from 0 to 3.1% on Cu/MC. Byproducts include ethyl acetate, methyl ethyl ketone, acetone, 1-butanol, butanal, and C6+, which are created by the cross- and self-aldol condensation of butanal and acetaldehyde.[42] These results demonstrate clearly that acetaldehyde appears as the primary product and the others are obtained in the secondary reactions. On the basis of these data, it was concluded that the acetaldehyde formed in a primary step was transformed successively to C3 or C4 oxygen-containing components by aldolization and ketonization. This tendency of Cu/SBA-15 is the same as that of the carbon-supported catalyst. However, the selectivity to acetaldehyde on the SiO_2-based catalyst is lower than that on Cu/MC. As the active sites on both Cu-based MC and SBA-15 catalysts are identical (Figure 5), the different product distributions are attributed to the diverse surface nature of the supports. Generally, the difference between them is the amount of oxygenic groups of the supports. On the surface of SBA-15 there are numerous –OH groups, the only type of oxygen-containing groups, ≈1.0 ± 0.1 nm^2,[43,44] which survive in isolated silanol groups: Si–OH.[45] However, the surface of the carbon material, pyrolyzed at 1073 K, contains ≈0.04 –COOH and –OH groups per nm^2 in addition to few other oxygenic units such as O–C=O.[35,46] Furthermore, the mass fraction of oxygen on mesoporous silica SBA-15 is 53.3 wt%, which is much higher than that on MC of 3.4 wt%.[47] Hence, on the basis of these results, we consider that the different amounts of –OH and/or –COOH groups on support surfaces lead to the significant distinction between Cu/MC and Cu/SBA-15 on acetaldehyde selectivity.

We combined our results with those in the literature to propose a possible schematic model of the reaction pathway of ethanol dehydrogenation on MC- and silica-supported Cu catalysts (Figure 7). To exhibit this difference vividly, the scarce surface groups on the carbon support, ≈0.04 –COOH and –OH groups per nm^2, are not shown. The secondary reactions are

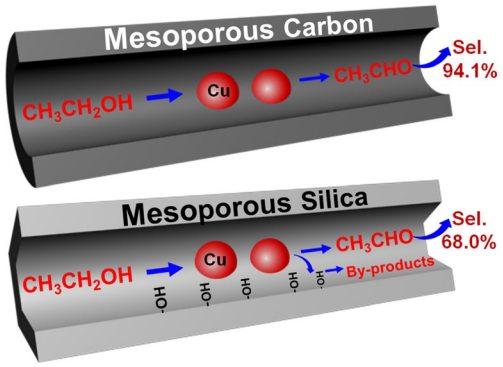

Figure 7. Scheme of C_2H_5OH conversion on Cu/MC and Cu/SBA-15.

catalyzed by Si–OH on the surface of the SBA-15 support. As a result, the selectivity to acetic aldehyde on Cu/MC is higher than that of Cu/SBA-15.

Conclusions

Cu nanoparticles supported on mesoporous carbon (MC) is an active catalyst for the dehydrogenation of ethanol to acetaldehyde with excellent selectivity compared with Cu/SBA-15. The reaction rate over Cu/MC was 1.7 times as high as that of Cu/SBA-15 at 553 K with a C_2H_5OH/N_2 molar ratio of 5:95 and a gaseous hourly space velocity (GHSV) of 26000 h^{-1}. A decrease of the GHSV and an increase of the reactant concentrations led to a selectivity of 94% and a space time yield of 225 h^{-1} at 553 K and a GHSV of 8600 h^{-1} over the carbon-supported Cu catalyst, whereas a selectivity of 68% and an output of 112 h^{-1} were obtained for Cu/SBA-15. A series of studies were employed to explore the structure–activity relationship of the catalysts. The high reaction rate of Cu/MC is attributed to the strong enrichment ability of the carbon support for ethanol molecules. Kinetic measurements show that the essence of the active sites is the same for the carbon- and silica-supported catalysts, and the difference in acetaldehyde selectivity is ascribed to the nature of the supports. The dependence of product selectivity and ethanol conversion on residence time suggests that abundant surface Si–OH groups of SBA-15 promote the secondary reactions, which are largely responsible for the low acetaldehyde selectivity of Cu/SBA-15. Conversely, side reactions are minimized on the carbon-supported Cu catalyst. Potentially, such a mesoporous carbon support with a unique nanostructure can be a promising candidate for the preparation of highly selective catalysts for ethanol dehydrogenation.

Experimental Section

Preparation of supports and catalysts

Resorcinol (99.5%) and formalin (37 wt% formaldehyde) were purchased from Tianjin Kermel Chemical Reagent Co., Ltd. 1,6-Diaminohexane (DAH, 99.0%), Cu(II) nitrate trihydrate (>99.0%), and ethanol (99.7%) were supplied by Sinopharm Chemical Reagent Co., Ltd. Pluronic F127 was purchased from Fluka. All chemicals were used as received. Mesoporous silica SBA-15 was synthesized according to a previous report.[32]

MC was prepared using a procedure reported previously.[48] Typically, resorcinol (24 g) and Pluronic F127 (10 g) were dissolved in a solvent mixture of ethanol (90 mL) and deionized water (72 mL) at 298 K. Afterward, 1,6-diaminohexane (1.247 g) was added to the above solution, which was stirred for ≈30 min at 298 K. Subsequently, formalin (32.6 mL) was injected quickly into the solution. After it was stirred at 298 K for another 10 min, the white homogeneous emulsion was then sealed in a flask and transferred to an oven at 363 K for 4 h. The as-made polymer monolith was dried at 323 K for 24 h, followed by pyrolysis at 1073 K for 2 h under N_2 atmosphere to obtain MC. Before catalyst preparation, MC was dried at 393 K for 2 h in a clean vial to eliminate water. Cu/MC with 10 wt% of Cu was prepared by incipient wetness impregnation with a $Cu(NO_3)_2{\cdot}3H_2O$ aqueous solution (0.625 g mL^{-1}). After impregnation, the catalyst precursors were kept at 298 K for 30 min followed by drying at 323 K for 12 h. Catalysts were reduced by 10 vol% H_2 at 723 K for 2 h before reaction. For comparison, 10 wt% Cu/SBA-15 was also prepared using the same method.

Catalyst characterization

The in situ XRD measurements of Cu/MC were performed by using a Panalytical X'pert Pro Super X-ray diffractometer using $Cu_{K\alpha}$ radiation ($\lambda = 0.15418$ nm) with a scanning angle (2θ) of 30–80°. The tube voltage was 40 kV, and the current was 40 mA. Typically, Cu/MC catalyst precursor was placed in a stainless-steel holder. Then a 5 vol% H_2/Ar mixture was introduced at a flow rate of 30 mL min^{-1}. Temperature ramping programs were performed from RT to 423, 523, 623, 723, and 823 K at a rate of 5 K min^{-1}. The XRD patterns were collected after samples reached the preset temperatures for 30 min. The XRD pattern of Cu/SBA-15 after reduction at 723 K for 2 h was obtained by using a D/MAX-2400 diffractometer using $Cu_{K\alpha}$ radiation (40 kV, 40 mA, $\lambda = 0.154056$ nm).

Nitrogen adsorption–desorption isotherms were measured by using a TriStar 3000 adsorption analyzer (Micromeritics) at 77.4 K. The supports were degassed at 473 K for 4 h before analysis, and reduced samples were degassed at 363 K for 4 h. The BET method was used to calculate the specific surface areas (S_{BET}). Total pore volumes (V_{total}) were calculated from the amount adsorbed at a relative pressure P/P_0 of 0.99. Pore size distributions (PSDs) were determined from the adsorption branches of the isotherms using DFT.

TEM and HRTEM measurements were conducted by using a Tecnai G^2 20 S-Twin microscope with an acceleration voltage of 200 kV.

The reducibility of 10 wt% Cu/MC and 10 wt% Cu/SBA-15 was determined by H_2-TPR by using a Micromeritics Autochem II 2920 instrument. Catalyst precursors (100 mg) were loaded into a quartz tube and dried in an argon stream at 373 K for 30 min before reduction to drive off water adsorbed physically. After it was cooled to 350 K, the sample was then heated in 30 mL min^{-1} of 8 vol% H_2/Ar at a rate of 10 K min^{-1} to 950 K. The amount of H_2 consumed during the run was detected by using a thermal conductivity detector (TCD).

A H_2-N_2O titration method was used to measure the Cu dispersion and average particle diameter in three processes.[49] First, the sample was reduced with 8 vol% H_2/Ar at 723 K for 2 h. The first H_2 consumption X at 350–650 K was collected. This H_2 consumption provides the total number of Cu atoms. It was confirmed that no further H_2 consumption was observed at a higher temperature by the reduction of Cu^{2+} to Cu. Second, the catalyst was cooled to 363 K, and 5 vol% N_2O/He was purged to the sample for 30 min for the oxidation of metallic Cu to cuprous oxide. Third, the second H_2-TPR was conducted from 313–573 K to reduce Cu^+ to Cu to obtain the second H_2 consumption Y. The dispersion was calculated by $D\,[\%] = 2Y/X \times 100$.[50]

Catalytic tests

DHEA was performed in a fixed-bed quartz tube reactor (i.d. 8 mm) under atmospheric pressure. Typically, catalyst (100 mg) was placed in the central zone of the reactor. Before the reaction, the catalyst was pretreated by in situ TPR from RT to 723 K for 2 h at a rate of 5 K min^{-1} using 10 vol% H_2 in N_2 (44 mL min^{-1} in total). When the temperature decreased to 373 K, ethanol (WHSV = 2.4 h^{-1}) was introduced into the evaporator (373 K) by using a syringe pump and carried into the reactor by flowing nitrogen gas

with a total flow rate of 40 mL min^{-1} ($C_2H_5OH/N_2 = 5:95$, molar ratio). The product line was heated at 393 K before a cold trap to remove the condensed liquid products. A GC7900 GC fitted with a FFAP capillary column (30 m, 0.32 mm, 0.5 μm) and a flame ionization detector (FID) was connected to the line between the reactor outlet and cold trap to analyze the products in the effluent gas. After the cold trap, the dry gas was detected by a TCD equipped with molecular sieves 5 Å and GDX-102 columns for the analysis of gas products (e.g., C_2H_4, CH_4, and others). CH_4 was used to bridge FID and TCD. The carbon balance of these reactions is more than 96% [Eqs. (1) and (2)].

$$\text{Ethanol conversion} = (\text{Ethanol}_{in} - \text{Ethanol}_{out})/\text{Ethanol}_{in} \times 100\,\% \quad (1)$$

$$\text{Product selectivity} = \text{Carbon in given product}/\text{Carbon in all products} \times 100\,\% \quad (2)$$

Acknowledgements

This project was financially supported by the National Natural Science Foundation for Distinguished Young Scholars (No. 21225312), the National Natural Science Foundation of China (No. 21403027), and the Fundamental Research Funds for the Central Universities (DUT14ZD209).

Keywords: carbon · copper · dehydrogenation · mesoporous materials · supported catalysts

[1] G. W. Huber, S. Iborra, A. Corma, *Chem. Rev.* **2006**, *106*, 4044 – 4098.
[2] P. Gallezot, *Chem. Soc. Rev.* **2012**, *41*, 1538 – 1558.
[3] J. Rass-Hansen, H. Falsig, B. Jørgensen, C. H. Christensen, *J. Chem. Technol. Biotechnol.* **2007**, *82*, 329 – 333.
[4] J. Mielby, J. Abildstrøm, F. Wang, T. Kasama, C. Weidenthaler, S. Kegnæs, *Angew. Chem. Int. Ed.* **2014**, *53*, 12513 – 12516; *Angew. Chem. Int. Ed.* **2014**, *126*, 12721 – 12724.
[5] OECD-FAO *Agricultural Outlook* 2013, OECD Publishing, Paris, **2013**.
[6] C. Angelici, B. M. Weckhuysen, P. C. Bruijnincx, *ChemSusChem* **2013**, *6*, 1595 – 1614.
[7] E. V. Makshina, M. Dusselier, W. Janssens, J. Degrève, P. A. Jacobs, B. F. Sels, *Chem. Soc. Rev.* **2014**, *43*, 7917 – 7953.
[8] V. I. Sobolev, K. Koltunov, O. A. Simakova, A. R. Leino, D. Murzin, *Appl. Catal. A* **2012**, *433 – 434*, 88 – 95.
[9] T. Takei, N. Iguchi, M. Haruta, *Catal. Surv. Asia* **2011**, *15*, 80 – 88.
[10] A. G. Sato, D. P. Volanti, D. M. Meira, S. Damyanova, E. Longo, J. M. C. Bueno, *J. Catal.* **2013**, *307*, 1 – 17.
[11] R. Prasad, *Mater. Lett.* **2005**, *59*, 3945 – 3949.
[12] S.-i. Fujita, N. Iwasa, H. Tani, W. Nomura, M. Arai, N. Takezawa, *React. Kinet. Catal. Lett.* **2001**, *73*, 367 – 372.
[13] P. Liu, E. J. M. Hensen, *J. Am. Chem. Soc.* **2013**, *135*, 14032 – 14035.
[14] C. Caro, K. Thirunavukkarasu, M. Anilkumar, N. R. Shiju, G. Rothenberg, *Adv. Synth. Catal.* **2012**, *354*, 1327 – 1336.
[15] V. L. Sushkevich, I. I. Ivanova, E. Taarning, *ChemCatChem* **2013**, *5*, 2367 – 2373.
[16] J. Bauer, G. M. Veith, L. F. Allard, Y. Oyola, S. H. Overbury, S. Dai, *ACS Catal.* **2012**, *2*, 2537 – 2546.
[17] J. Keuler, PhD thesis, University of Stellenbosch, South Africa, **2000**.
[18] Y. Zhang, Master's thesis, Tianjin University, China, **2007**.
[19] A. G. Sato, D. P. Volanti, I. C. D. Freitas, E. Longo, J. Bueno, *Catal. Commun.* **2012**, *26*, 122 – 126.
[20] J. Scalbert, F. Thibault-Starzyk, R. Jacquot, D. Morvan, F. Meunier, *J. Catal.* **2014**, *311*, 28 – 32.
[21] T. Nishiguchi, T. Matsumoto, H. Kanai, K. Utani, Y. Matsumura, W.-J. Shen, S. Imamura, *Appl. Catal. A* **2005**, *279*, 273 – 277.
[22] M. Iwamoto, M. Tanaka, S. Hirakawa, S. Mizuno, M. Kurosawa, *ACS Catal.* **2014**, *4*, 3463 – 3469.
[23] R. Lv, T. Cui, M.-S. Jun, Q. Zhang, A. Cao, D. S. Su, Z. Zhang, S.-H. Yoon, J. Miyawaki, I. Mochida, F. Kang, *Adv. Funct. Mater.* **2011**, *21*, 999 – 1006.
[24] D. Su, S. Perathoner, G. Centi, *Chem. Rev.* **2013**, *113*, 5782 – 5816.
[25] S. Wang, Q. Zhao, H. Wei, J. Q. Wang, M. Cho, H. Cho, O. Terasaki, Y. Wan, *J. Am. Chem. Soc.* **2013**, *135*, 11849 – 11860.
[26] Z. Y. Jin, A. H. Lu, Y. Y. Xu, J. T. Zhang, W. C. Li, *Adv. Mater.* **2014**, *26*, 3700 – 3705.
[27] G. P. Hao, Z. Y. Jin, Q. Sun, X. Q. Zhang, J. T. Zhang, A. H. Lu, *Energy Environ. Sci.* **2013**, *6*, 3740 – 3747.
[28] Y. Zhang, A. Wang, T. Zhang, *Chem. Commun.* **2010**, *46*, 862 – 864.
[29] K. I. Choi, M. Vannice, *J. Catal.* **1991**, *131*, 22 – 35.
[30] S. Zhao, H. Yue, Y. Zhao, B. Wang, Y. Geng, J. Lv, S. Wang, J. Gong, X. Ma, *J. Catal.* **2013**, *297*, 142 – 150.
[31] F. W. Chang, H. C. Yang, L. Roselin, W. Y. Kuo, *Appl. Catal. A* **2006**, *304*, 30 – 39.
[32] D. Zhao, J. Feng, Q. Huo, N. Melosh, G. H. Fredrickson, B. F. Chmelka, G. D. Stucky, *Science* **1998**, *279*, 548 – 552.
[33] I. Kvande, D. Chen, M. Rønning, H. J. Venvik, A. Holmen, *Catal. Today* **2005**, *100*, 391 – 395.
[34] A. Dandekar, R. T. K. Baker, M. A. Vannice, *J. Catal.* **1999**, *183*, 131 – 154.
[35] D. C. Guo, J. Mi, G. P. Hao, W. Dong, G. Xiong, W. C. Li, A. H. Lu, *Energy Environ. Sci.* **2013**, *6*, 652 – 659.
[36] K. H. Chuang, C. Y. Lu, M. Y. Wey, Y. N. Huang, *Appl. Catal. A* **2011**, *397*, 234 – 240.
[37] Z. He, H. Lin, P. He, Y. Yuan, *J. Catal.* **2011**, *277*, 54 – 63.
[38] D. H. Nam, J. H. Lee, N. R. Kim, Y. Y. Lee, H. W. Yeon, S. Y. Lee, Y. C. Joo, *Carbon* **2015**, *82*, 273 – 281.
[39] N. Kanoun, M. P. Astier, G. M. Pajonk, *Appl. Catal.* **1991**, *70*, 225 – 236.
[40] N. Kanoun, M. P. Astier, G. M. Pajonk, *J. Mol. Catal.* **1993**, *79*, 217 – 228.
[41] M. J. L. Gines, E. Iglesia, *J. Catal.* **1998**, *176*, 155 – 172.
[42] V. L. Sushkevich, I. I. Ivanova, V. V. Ordomsky, E. Taarning, *ChemSusChem* **2014**, *7*, 2527 – 2536.
[43] S. W. Song, K. Hidajat, S. Kawi, *Langmuir* **2005**, *21*, 9568 – 9575.
[44] K. Fujdala, T. Tilley, *J. Am. Chem. Soc.* **2001**, *123*, 10133 – 10134.
[45] M. A. Natal-Santiago, J. A. Dumesic, *J. Catal.* **1998**, *175*, 252 – 268.
[46] G. P. Hao, F. Han, D. C. Guo, R. J. Fan, G. Xiong, W. C. Li, A. H. Lu, *J. Phys. Chem. C* **2012**, *116*, 10303 – 10311.
[47] G. P. Hao, W. C. Li, D. Qian, A.-H. Lu, *Adv. Mater.* **2010**, *22*, 853 – 857.
[48] G. P. Hao, W.-C. Li, D. Qian, G.-H. Wang, W.-P. Zhang, T. Zhang, A.-Q. Wang, F. Schüth, H.-J. Bongard, A.-H. Lu, *J. Am. Chem. Soc.* **2011**, *133*, 11378 – 11388.
[49] A. Gervasini, S. Bennici, *Appl. Catal. A* **2005**, *281*, 199 – 205.
[50] E. D. Guerreiro, O. F. Gorriz, G. Larsen, L. Arrúa, *Appl. Catal. A* **2000**, *204*, 33 – 48.

Received: May 5, 2015
Published online on August 6, 2015